Research Square

Preprints are preliminary reports that have not undergone peer review.
They should not be considered conclusive, used to inform clinical practice,
or referenced by the media as validated information.

Clean-Reference Spatial Filtering for Selective Stroke- Volume Recovery in Electrical Impedance Tomography

Junhyeok Choi
Handong Global University
Daeun Gwon
Handong Global University
Sung Hyun Hong
BiLab
Minkyu Ahn
minkyuahn@handong.edu

Handong Global University

Article

Keywords: Electrical impedance tomography, cardiac monitoring, motion artifact suppression, principal component analysis, spatial filtering, stroke volume

Posted Date: July 31st, 2026

DOI: https://doi.org/10.21203/rs.3.rs-10215722/v1

License: This work is licensed under a Creative Commons Attribution 4.0 International License.
Read Full License

Additional Declarations: No competing interests reported.

Clean-Reference Spatial Filtering for Selective Stroke-Volume Recovery in Electrical Impedance Tomography

Authors: Junhyeok Choi[1], Daeun Gwon[2,3], Sung Hyun Hong[4], Minkyu Ahn[1,2,5*]

Affiliations:

[1]Department of Artificial Intelligence, Computer Science and Engineering, Handong Global University, Pohang, Republic of Korea

[2]Institute for Information and Communication Technology, Handong Global University, Pohang, Republic of Korea

[3]Department of Neuroscience, Johns Hopkins University School of Medicine, Baltimore, MD, USA

[4]Institute for Information and Communication Technology, Handong Global University, Pohang, Republic of Korea

[5]School of Artificial Intelligence, Computer Science and Engineering, Handong Global University, Pohang, Republic of Korea

Correspondence: Minkyu Ahn (minkyuahn@handong.edu)

Submitted to Scientific Reports

Clean-Reference Spatial Filtering for Selective Stroke-Volume Recovery in Electrical Impedance Tomography

Keywords: Electrical impedance tomography, cardiac monitoring, motion artifact suppression, principal component analysis, spatial filtering, stroke volume

Abstract

Motion can distort cardiac electrical impedance tomography (EIT) and reduce the reliability of short-window stroke-volume (SV) estimation. We evaluated whether a nearby motion-free EIT segment can provide a local clean reference for suppressing a motion-contaminated cardiac EIT. Six clinical recordings with synchronized EIT, electrocardiography (ECG), and clinical-reference SV were analyzed. For each motion-contaminated target window, a principal component analysis (PCA) spatial basis was estimated from the preceding clean segment and the target was projected onto this basis before standard ECG-guided cardiac extraction. In 2,963 complete-case clinical-reference SV observations from the clean10-motion20 endpoint, clean-reference PCA reduced the median SV error from 8.28 mL to 7.83 mL compared with window-wise principal component analysis-independent component analysis (PCA-ICA), with subject-level median improvement in all six recordings. The benefit was concentrated on the high-baseline-error windows, whereas some already-low-error windows worsened. A 10 s clean reference did not show a clear loss relative to 20 s on matched targets and increased detector-level clean-reference availability. Local clean-reference PCA may therefore be useful as a reference-guided recovery strategy for motion-contaminated cardiac EIT, but the validation of new recordings and the reference-independent quality gating are required before routine use.

Introduction

Electrical impedance tomography (EIT) is a noninvasive, high-temporal-resolution modality for cardiopulmonary monitoring.[1–4] EIT reconstructs internal resistivity changes by injecting small alternating currents through chest-surface electrodes that enable bedside tracking of dynamic cardiopulmonary physiology. Although EIT has been used most widely for ventilation monitoring, its temporal resolution and noninvasive acquisition have also motivated cardiac applications, including relative stroke-volume (SV) estimation.

Cardiac EIT is particularly vulnerable to motion artifacts because cardiac-related impedance variation is small relative to impedance changes caused by body movements, electrode displacements, and electrode-skin contact variations. This problem is amplified in short-window analyses, where beat-level hemodynamic estimation is required but the available signal duration is limited. Motion artifacts in EIT can include baseline drift, step-like changes, and spike-like disturbances driven by contact impedance changes and body movements. [5]

Prior cardiac EIT studies have commonly used spatial filtering based on principal component analysis (PCA) and independent component analysis (ICA), estimated during a calibration period and then applied to subsequent data.[6-9] These studies demonstrated separation of respiratory and cardiac components, real-time spatial filtering, and EIT-derived SV comparisons against invasive or less invasive hemodynamic references. This strategy is effective when the calibration segment represents later signal structure, but a single calibration-time spatial filter may generalize poorly when motion or posture changes alter the apparent spatial distribution of cardiac-related impedance changes.

Wavelet-based and adaptive filtering approaches have also been proposed for EIT motion-artifact suppression.[5, 10] However, many evaluations have focused on ventilation EIT or synthetic artifact models rather than prolonged clinical cardiac EIT recordings with external SV references. In such recordings, long representative calibration intervals may be difficult to identify, and artifact-dominated target windows can destabilize window-wise decomposition.

A temporally adjacent clean segment offers an alternative local reference: PCA can estimate recently observed clean spatial modes without requiring a fixed prior model. Clean-reference subspace estimation has also been used in other biomedical modalities, such as artifact subspace reconstruction in electroencephalography and component-based noise correction in functional magnetic resonance imaging.[11, 12] The proposed method adapts this idea to cardiac EIT by projecting a motion-contaminated target onto the spatial subspace observed during a nearby clean cardiac segment, rather than attempting to identify the artifact components directly.

The present study evaluates this local clean-reference principle for motion-contaminated cardiac EIT. For each motion target window, the preceding clean segment was used to estimate a PCA subspace, and the motion target was projected onto that subspace before standard cardiac signal extraction.

We tested two hypotheses: H1, CleanRef-PC1-10, is defined as clean-reference PCA retaining principal components (PCs) 1–10. It reduces clinical-reference SV error relative to window-wise PCA-ICA across motion-detected windows. H1's practical benefit is concentrated in high-baseline-error windows, whereas already-low-error windows require maintenance and over-filtering-risk

characterization. H2 is a 10 s clean reference that shows no sign of inferiority relative to 20 s on matched motion targets.

The clinical reference devices were treated as clinically used hemodynamic channels that are not error-free gold standards.[13-15] Therefore, mL-scale SV results are interpreted as relative agreement comparisons under a shared subject-level scale and not as validation of standalone SV measurement in new recordings.

Results

For orientation, clean10-motion20 and clean20-motion20 denote 20 s motion target windows paired with preceding 10 s or 20 s clean reference segments, respectively. WW-PCAICA denotes the standard window-wise PCA-ICA extraction pipeline applied directly to the target window. FixedCal-PCAICA denotes a single retrospective calibration-style PCA-ICA filter per recording. CleanRef-PC1-10 denotes clean-reference PCA projection using clean-segment PCs 1-10 before the same ECG-guided cardiac extraction pipeline.

The primary endpoint was a paired absolute SV error relative to the clinical-reference SV after applying one shared subject-level scale across methods. Cohort A was used for matched clean10-vs-clean20 feasibility, Cohort B for the primary all-comers clean10-motion20 SV comparison, and Cohort C for the clean20-clean20 no-motion reliability baseline.

In the tables and figures, the acronyms are root-mean-square (RMS), interquartile range (IQR), cardiac volume signal (CVS), normalized cross-correlation (xcorr), and normalized root-mean-square error (NRMSE). The overall windowing, clean-reference projection, and ECG-guided cardiac extraction workflow are summarized in Figure 1.

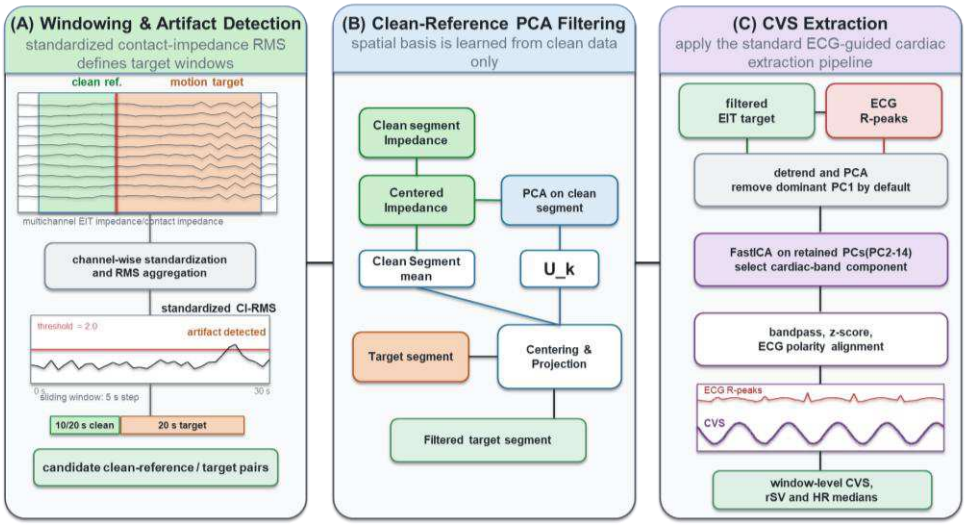


Figure 1. Clean-reference PCA pipeline for motion-contaminated cardiac EIT. Sliding windows were formed from multichannel EIT/contact-impedance data, artifact-positive targets were paired with preceding clean references, and clean-reference PCA projection was applied before ECG-guided cardiac extraction.

Window Composition

Under RMS = 2.0, the dataset contained 3,919 detected 20 s motion windows. Of these, 1,413 had a preceding 10 s clean segment and 892 had a preceding 20 s clean segment. Shortening the clean-

reference requirement increased candidate availability, especially in recordings with sparse clean intervals. S1 had only one 20 s clean-eligible window, but it had 66 windows under the 10 s clean criterion. These counts describe detector-level clean-reference availability and are not the denominators for the endpoint-specific complete-case analyses below.

Table 1. Detector-level window composition by subject. Counts summarize target-only detector diagnostics before endpoint-specific complete-case filtering and are not the denominators for Tables 2–4.

Subject	Total 20s	Clean 20s	Detected20	With preceding 10 s clean	With preceding 20 s clean	Total 10s	Clean 10s	Motion 10s
S1	484	1	483	66	1	486	68	418
S2	469	263	206	90	69	471	312	159
S3	504	37	467	54	13	506	84	422
S4	3,478	1,731	1,747	788	482	3,480	2,230	1,250
S5	3,009	2,062	947	370	293	3,011	2,274	737
S6	2,489	2,420	69	45	34	2,491	2,446	45
Total	10,433	6,514	3,919	1,413	892	10,445	7,414	3,031

All-comers SV improvement and fixed-calibration comparison

In the primary all-comers Cohort B, 2,963 complete-case clinical-reference SV observations had finite clinical-reference SV errors for WW-PCAICA, fixedCal-PCAICA, and CleanRef-PC1-10. WW-PCAICA had a median SV error of 8.28 mL. CleanRef-PC1-10 reduced its median SV error to 7.83 mL, with paired median Δ = −0.43 mL and 53.6% of windows improved. Subject-level median SV error improved in all six SV-evaluable recordings, indicating that this improvement trend was not driven solely by high-window-count subjects.

FixedCal-PCAICA performed poorly under the present frequent-motion conditions. Median SV error was 21.93 mL, with paired median Δ = +13.02 mL versus WW-PCAICA. Only 21.4% of paired windows improved, and subject-level improvement occurred in 0/6 recordings. This supports the need for local adaptation in this dataset, without refuting prior calibration-style approaches in their original controlled settings.

Table 2. All-comers clinical-reference SV comparison using complete-case Cohort B observations.

Method	Complete-case N	Median SV Error (mL)	IQR (mL)	Median Δ vs WW-PCAICA (mL)	Improved (%)	Subjects Improved
WW-PCAICA	2,963	8.279	3.817–15.829	0.000	Reference	Reference
FixedCal-PCAICA	2,963	21.932	14.219–29.339	+13.024	21.4	0/6
CleanRef-PC1-10	2,963	7.829	3.659–13.504	-0.425	53.6	6/6

Note: Supportive waveform metrics for the same paired comparison are reported in Supplementary Table S14.

Baseline-error-dependent response

The all-comers improvement was not uniform. When Cohort B was stratified by WW-PCAICA SV-error tertiles, the lower tertile showed low baseline error and a positive paired median Δ (+1.77 mL), indicating over-filtering risk when the baseline estimate was already accurate. The middle tertile

showed a small improvement (−0.51 mL). The upper tertile showed the largest practical recovery, with paired median Δ = −8.61 mL and 76.6% of windows improved.

Already-low-error maintenance was also assessed. Among windows with WW-PCAICA SV error ≤10 mL, 1311/1705 (76.9%) remained ≤10 mL after CleanRef-PC1-10 filtering. However, large worsening occurred in 17.3% of all windows for ΔSV error > +5 mL and 7.5% for ΔSV error > +10 mL. These results support selective rather than unconditional filtering: CleanRef-PC1-10 is most useful where baseline PCA-ICA agreement is poor, but it can worsen some already-low-error windows.

Figure 2 visualizes this asymmetric response. Most large negative deltas occurred in windows with high WW-PCAICA SV error, whereas low-baseline-error windows clustered near zero or positive deltas. Because baseline SV error requires clinical-reference SV, it cannot serve as a deployment trigger. The stratified analysis identifies where filtering helped retrospectively and motivates future signal-quality-aware gating using reference-SV-independent proxies, such as ECG-locked CVS xcorr, NRMSE, contact-impedance RMS, cardiac-band power, or decomposition stability.

Table 3. Baseline-error-stratified all-comers SV response to CleanRef-PC1-10 filtering.

Baseline SV-error stratum	N	WW-PCAICA SV err	CleanRef-PC1-10 SV err	Paired Δ	Improved %	Large worsening >5 mL	Large worsening >10 mL
Lower tertile	988	2.492 [1.236-3.817]	4.151 [1.852-8.170]	+1.765 [-0.356-5.429]	30.2	26.7	11.8
Middle tertile	987	8.279 [6.670-10.198]	7.694 [4.507-11.638]	-0.506 [-3.596-2.889]	54.0	15.2	5.5
Upper tertile	988	23.980 [15.829-39.648]	13.158 [7.516-21.611]	-8.611 [-21.509--0.490]	76.6	10.0	5.1

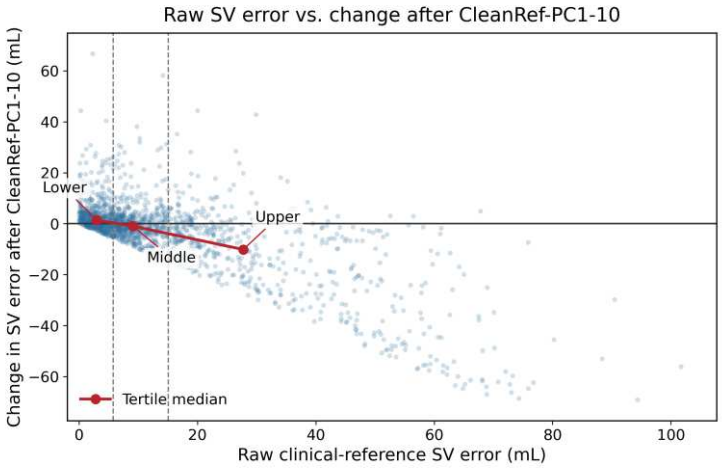


Figure 2. Baseline SV error versus SV-error change after filtering. Negative values indicate improved clinical-reference SV agreement after CleanRef-PC1-10, with the largest recovery concentrated in high-baseline-error windows.

Clean10 vs clean20 feasibility

Clean-reference duration was tested on Cohort A by comparing 10 s and 20 s clean-reference PCA bases applied to identical 20 s motion targets. Both filtered methods outperformed WW-PCAICA. WW-PCAICA median SV error was 9.12 mL, CleanRef-PC1-10/c10 was 7.94 mL, and CleanRef-PC1-10/c20 was 7.85 mL.

In a direct paired comparison, clean10 showed no signal of inferiority relative to clean20: SV error 7.92 versus 7.79 mL (p = 0.696), xcorr 0.873 versus 0.867 (p = 0.833), and NRMSE 0.456 versus 0.458 (p = 0.316). This should be interpreted as practical feasibility, not confirmatory, noninferiority, or interchangeability.

Spatial-basis analysis supported this result (Figure 3). At k = 10, clean20-vs-clean10_last similarity exceeded clean20-vs-motion20 similarity across projector similarity, mean canonical correlation, and |PC1 dot|. Median |PC1 dot| was approximately 0.998, indicating near-identical dominant spatial modes. Higher-order PCs showed more reordering, but the dominant basis structure was preserved (Figure 3B).

Table 4 isolates the head-to-head duration effect by comparing clean10- and clean20-trained filters on the same target windows. Negative SV/NRMSE deltas favor clean20; positive xcorr deltas favor clean20. Full pooled method values and subject-level summaries are reported in the Supplementary Information.

Table 4. Direct paired clean10-vs-clean20 comparison on matched clean20-motion20 targets. N denotes window-level complete-case pairs for each metric. SV N differs from xcorr/NRMSE N because SV required finite clinical-reference matching and scaling, whereas morphology metrics did not.

Metric	N	clean10	clean20	Paired Median Δ (c20−c10)	p
SV	1,664	7.916	7.787	-0.0434	0.696
xcorr	1,826	0.873	0.867	-0.000202	0.833
NRMSE	1,826	0.456	0.458	+0.00246	0.316

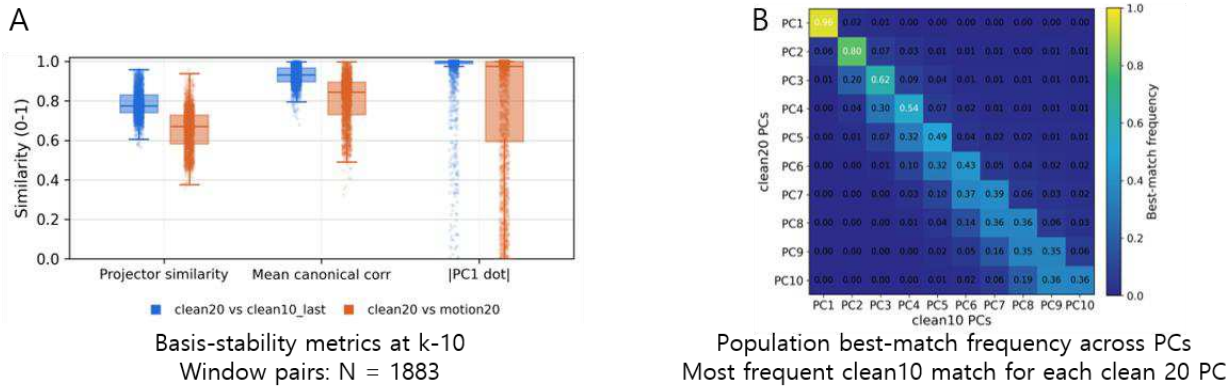


Figure 3. Clean20 versus clean10 spatial-basis similarity. Clean10 retained the dominant clean-reference spatial structure relative to clean20, while clean-vs-motion comparisons showed larger basis differences.

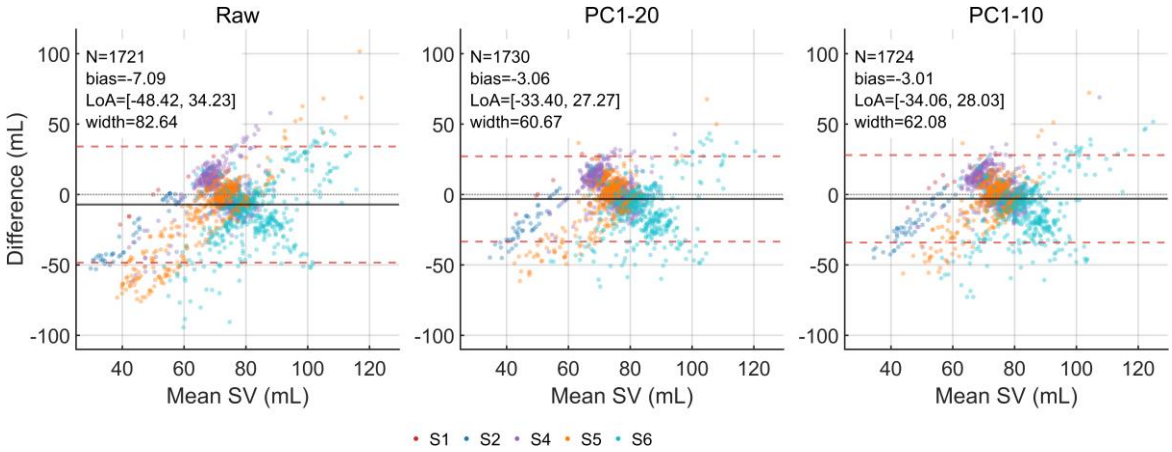


Figure 4. Bland-Altman SV agreement for WW-PCAICA and clean-reference PCA. Clean-reference PCA narrowed descriptive limits-of-agreement width relative to WW-PCAICA, but remaining dispersion does not establish clinical interchangeability.

Figure 4 places the SV-error findings in an agreement-analysis view.[16] Bland-Altman summaries showed narrower limits of agreement after clean-reference PCA, supporting reduced agreement dispersion in addition to the median-error shift. Limits-of-agreement width narrowed from 82.65 mL with WW-PCAICA to 60.67 mL with CleanRef-PC1-10/c20 and 62.08 mL with CleanRef-PC1-10/c10. However, the remaining spread was substantial; therefore, these plots were interpreted descriptively and do not establish clinical interchangeability.

Clean10-only operational gain

Shortening the clean-reference criterion increased detector-level operational coverage. Across subjects, 1,413 detected motion targets had a preceding 10 s clean segment, whereas 892 also had a preceding 20 s clean segment; 521 candidate windows were therefore available only under the 10 s criterion. Endpoint-level clean10-only performance was evaluated using the same complete-case definitions as the primary SV analysis. The clean10-only subset showed median SV-error reduction relative to WW-PCAICA (paired median $\Delta = -0.29$ mL; 52.4% improved). The clean20-eligible subset showed a larger reduction (paired median $\Delta = -0.71$ mL; 55.7% improved), but the clean10-only result supports the practical value of retaining windows that would otherwise be excluded. Detailed clean10-only subset values are provided in Supplementary Table S5.

Sensitivity and supporting analyses.

PC-range sensitivity distinguished two design dimensions: the clean-reference PCA projection subspace and the downstream PCA-ICA PC1 policy. CleanRef-PC1-10 with downstream PC1 removed remained the primary configuration because all primary analyses were performed with this conservative setting. PC2-k rows were worse than the PC1-10 reference configuration, supporting PC2-k as a negative comparator. PC1-14 retained produced the best pooled all-comers value but was not subject-robust, improving 2/6 subjects and worsening 4/6 by paired median difference. It is therefore retained as a hypothesis-generating candidate.

The clean20-clean20 no-motion baseline showed low intrinsic variability (median SV intrinsic Delta = 0.199; xcorr 0.885 to 0.905), supporting the interpretation that motion-window changes exceeded pipeline-intrinsic variation. Clean-window reference agreement showed lower SV error than motion-window WW-PCAICA, and CleanRef-PC1-10 shifted motion-window agreement toward the clean-window baseline.

Detector-threshold endpoint sensitivity supported RMS = 2.0 as a balanced default threshold. CleanRef-PC1-10 had the lowest observed median SV error at RMS = 2.0 compared with 1.5, 2.5, and 3.0. The stricter 1.5 threshold yielded a larger paired median improvement but a much smaller paired set and omitted one SV-evaluable subject; looser thresholds reduced subject-level robustness. Detailed PC-range sensitivity values are provided in Supplementary Table S6. Detailed normalized, subject-level, detector-threshold, morphology-support and representative-window materials are provided in the Supplementary Information.

Discussion

Clean-reference PCA modestly improved clinical-reference SV agreement relative to WW-PCAICA across motion-detected windows. The pooled median reduction was small, but subject-level direction was consistent across all six SV-evaluable recordings. The result should be interpreted as relative agreement improvement against clinically used reference devices under retrospective shared scaling, not as proof of standalone mL accuracy.

The small pooled median effect is clinically and methodologically important to interpret in context. Motion-contaminated cardiac EIT windows are heterogeneous: some retain a recoverable cardiac component, others are already well-handled by window-wise decomposition, and still others may be too degraded for spatial projection to recover. Under this mixture, a large all-comers median shift would not be expected unless the filter helped nearly every window. The more relevant signal is that improvement was directionally consistent across recordings and concentrated in windows with poor baseline agreement. This pattern suggests that clean-reference PCA is not a general accuracy booster, but a local recovery mechanism for a subset of otherwise unreliable windows.

The most important finding is not the pooled median alone, but the error-dependent response pattern. High-baseline-error windows showed the largest practical recovery, whereas already-low-error windows had limited room to improve and a measurable risk of worsening. This supports a selective recovery interpretation: clean-reference PCA is most valuable when the baseline window-wise decomposition appears unreliable, but unconditional application to every motion-detected window is not optimal.

WW-PCAICA adapts to each target window by re-estimating PCA-ICA, but an artifact-dominated target can destabilize the decomposition. FixedCal-PCAICA applies one stable filter across time, but a single filter may not represent later motion-altered spatial distributions. CleanRef-PC1-10 represents an intermediate approach: It updates the spatial reference from a nearby clean segment while constraining the target to recently observed clean spatial modes. This may explain why it improved high-error windows and why fixedCal-PCAICA generalized poorly in these recordings.

The fixed-calibration result should be interpreted narrowly. The present recordings lacked a prospective calibration period, so the longest available clean segment was used as a surrogate. The poor fixedCal-PCAICA performance does not invalidate prior calibration-time PCA-ICA work in controlled settings; instead, it shows that a single retrospective fixed filter was not robust under the frequent-motion conditions of this dataset.

The clean10-vs-clean20 analysis supports the practical feasibility of a 10 s clean reference. Endpoint differences were small and statistically indistinguishable, dominant spatial modes were nearly

identical, and shortening the criterion recovered additional candidate windows. This is important because long clean intervals are not always available in clinical recordings. We interpret this conclusion cautiously. This was not a formal non-inferiority design, and clean10 should be validated prospectively before being treated as interchangeable with clean20.

The operational implication of the 10 s result is therefore not simply that shorter calibration is convenient. In bedside or prolonged recordings, clean intervals may occur in brief fragments between movement, care procedures, posture changes, or electrode-contact disturbances. Requiring 20 s of clean data can exclude recordings or time periods in which a shorter but spatially stable clean reference is available. The clean10-only analysis indicates that these additional windows were not merely numerically added. They retained measurable recovery relative to WW-PCAICA. This supports a workflow in which clean-reference projection is updated opportunistically from recent clean fragments rather than waiting for longer calibration intervals.

The baseline-error-dependent analysis is retrospective because baseline SV error requires clinical-reference SV. It is therefore not directly deployable. However, it clarifies the desired future operating behavior: apply projection when recovery potential is high and avoid it when WW-PCAICA output is already acceptable. Reference-SV-free signal-quality metrics may provide this gate. Candidate metrics include ECG-locked CVS xcorr and NRMSE relative to a clean CVS template, contact-impedance RMS, cardiac-band power, spectral residuals, and decomposition stability. These proxies require validation against clinically meaningful SV-error outcomes.

This gating requirement also reframes apparent failures. Worsening in already-low-error windows should not be treated only as a limitation of the projection. It also defines the boundary condition under which projection should be withheld. A practical implementation would first estimate whether the unfiltered or WW-PCAICA-derived cardiac waveform is unreliable, then apply clean-reference PCA only when expected recovery outweighs over-filtering risk. Future work should therefore evaluate the method as a decision policy and not only as a filter. Candidate gates should be trained without access to reference SV, tested on held-out recordings, and assessed using both recovery of high-error windows and preservation of low-error windows.

This study has several limitations. First, only six recordings were analyzed, with subject imbalance and heavily overlapping 5 s-step windows. Window-level p-values may overstate precision and are interpreted descriptively. Subject-level summaries provide a conservative check but remain underpowered. Second, clinical reference devices are not error-free gold standards and carry known measurement uncertainty relative to PAC-based references.[13-15] The observed SV-error reduction is small relative to that uncertainty. Third, mL-scale SV estimates used retrospective subject/recording-level scaling from WW-PCAICA windows. This enables fair method comparison under a shared scale but does not establish deployable mL-scale calibration. Fourth, the baseline-error gate is retrospective, and morphology-based proxy gates remain exploratory. Fifth, findings are specific to the HemoVista™ system (BiLab Inc., Seongnam-si, Republic of Korea) anterior cardiac configuration and require revalidation across other EIT systems, electrode configurations, and clinical cohorts. Sixth, alternative suppressors, such as DWT-based methods and deep-learning denoisers, were not directly compared.

In summary, clean-reference PCA improved relative clinical-reference SV agreement in motion-contaminated cardiac EIT, with the strongest practical benefit concentrated in high-baseline-error windows. Because already-low-error windows showed measurable over-filtering risk, the method should be developed as a selective recovery tool rather than an unconditional filter. The 10 s clean

reference appeared practically feasible and increased candidate availability, but future work should validate reference-SV-independent quality gates, prospective SV calibration, and performance in larger multi-device clinical cohorts.

Methods

Subjects

A total of six subjects (S1-S6) from two independent clinical studies were included in this study. The analyzed dataset consisted of three subjects from an intensive care unit (ICU) study and three subjects from an operating room (OR) study. The ICU dataset was included to evaluate the robustness of the proposed method against patient motion artifacts, whereas the OR dataset was included to evaluate its robustness against severe interference caused by surgical equipment.

The study protocols were approved by the Institutional Review Board (IRB) of Asan Medical Center (Approval Nos. KCT0008487 and KCT0009069). The experiments were conducted with the subjects' full understanding and their written informed consent. All procedures were performed in accordance with the relevant guidelines and regulations.

Clinical reference hemodynamic measurements were obtained using routine invasive monitoring systems. The ICU recordings used the HemoSphere system (Edwards Lifesciences, Irvine, CA, USA), whereas the OR recordings used the Vigileo system (Edwards Lifesciences, Irvine, CA, USA) or the PulsioFlex system (Getinge, Gothenburg, Sweden). Stroke volume values reported by these systems, or values derived from the recorded cardiac output and heart rate when only cardiac output was available, were used as the clinical reference for evaluation.

Data Acquisition

EIT was acquired at 100 Hz using the HemoVista™ system (BiLab Inc., Seongnam-si, Republic of Korea) with 16 anterior thoracic electrodes, two shared with ECG, which was acquired at 500 Hz. The reported spatial patterns are therefore specific to this cardiac-oriented anterior configuration and should not be generalized to circumferential pulmonary EIT belts without revalidation.

Signal Processing

A common ECG-guided pipeline generated cardiac volume signal (CVS), relative stroke volume (rSV), and heart rate (HR) for all methods. After per-channel detrending, singular value decomposition (SVD)-based PCA was applied to each analysis window. The first principal component (PC1) was treated as the dominant respiratory component and removed by default. Fast independent component analysis (FastICA)[17] was then applied to the remaining principal components (PCs), and the cardiac component was selected by maximum Welch power in the cardiac band (0.5-4 Hz). The selected component was then filtered with a sixth-order zero-phase IIR Butterworth bandpass filter using 0.5 and 15 Hz half-power cutoff frequencies at the 100 Hz EIT sampling rate, followed by z-scoring and ECG-guided polarity alignment. Beat-wise rSV was computed as the CVS valley-to-peak amplitude for each R-R interval, followed by amplitude-based and robust outlier rejection. Window-level rSV and HR were within-window medians. Cardiac output (CO) was excluded from the main analysis because it is derived from SV × HR and preliminary CO results closely followed the SV trends.

Clinical-reference SV scaling

Clinical-reference SV was matched to each EIT target window within ±10 s of the target-window center. When multiple reference samples were available, their median was used. The clinical devices provided low-rate hemodynamic reference values rather than beat-by-beat gold-standard measurements.

Because EIT-derived rSV is relative, mL-scale SV required retrospective scaling. For each subject/recording, one WW-PCAICA-derived scale factor was estimated from finite reference-matched WW-PCAICA windows: the median of RefSV/rSV. The same scale was then applied to WW-PCAICA, fixed-calibration PCA-ICA (fixedCal-PCAICA), and CleanRef-PC1-10. This shared-scale design avoids method-specific calibration advantages, but it does not establish deployable mL-scale calibration.

Motion detection and window cohorts

Motion was detected from standardized contact-impedance RMS after channel-wise normalization. The primary detector threshold was RMS = 2.0, selected from visual waveform inspection, candidate-count sensitivity, and endpoint-level sensitivity analysis. Sliding windows used a 5 s step. Candidate windows consisted of a clean reference segment followed by a 20 s target segment, using either 10 s or 20 s clean-reference duration.

Three cohorts were used. Cohort A was the matched clean20-motion20 set used for clean10-vs-clean20 feasibility. Cohort B was the all-comers clean10-motion20 set used for the primary SV comparison, fixedCal comparison, and baseline-error stratification. Cohort C was the clean20-clean20 no-motion reliability baseline.

Clean-reference PCA and comparators

For each candidate window, PCA was estimated from the clean segment only. Let $X_c \in R^{C \times T_c}$ denote the clean reference segment and $X_t \in R^{C \times T_t}$ denote the motion target segment, where C is the number of EIT channels and T_c and T_t are the numbers of clean-reference and target time samples, respectively. The clean-segment channel mean $\mu_c \in R^{C \times 1}$ was computed across time and subtracted from each time sample of both segments. Thus, the centered matrices were defined as $\hat{X}_c = X_c - \mu_c$ and $\hat{X}_t = X_t - \mu_c$.

PCA was implemented by singular value decomposition (SVD) of the centered clean-reference matrix, $\hat{X}_c = \mathrm{U}\Sigma\mathrm{V}^T$. The retained clean spatial basis was $W_k = U(:, 1{:}k)$, or the corresponding selected columns of U when an explicit PC index set was used. The motion target was then projected onto this clean-reference spatial subspace and reconstructed as $\tilde{X}_t = W_k W_k^T \hat{X}_t + \mu_c$.

The primary configuration, CleanRef-PC1-10, retained PCs 1-10 from the clean-reference SVD. After projection, the standard CVS/SV extraction pipeline was applied.

The main comparator was WW-PCAICA, defined as the standard window-wise PCA-ICA extraction pipeline applied directly to each target window without clean-reference projection. The second comparator was fixedCal-PCAICA, a retrospective calibration-style baseline modeled after prior real-time PCA-ICA spatial-filter studies. Because no separate prospective calibration period was available, the longest motion-free clean segment in each recording was used as a surrogate calibration segment. PCA-ICA parameters estimated once from that segment were then applied without updating

to subsequent target windows. This was a retrospective adaptation, not a replication of the original animal-study protocol.

Morphology, basis stability, and statistics

ECG-locked CVS morphology was evaluated by segmenting CVS beats between consecutive R-peaks, baseline-correcting and standardizing each beat, and comparing target beats with a clean CVS template. Pearson correlation, lag-restricted normalized cross-correlation (xcorr), and lag-aligned normalized root-mean-square error (NRMSE) were used as supportive morphology metrics.

To test whether 10 s clean references preserved the spatial structure of 20 s references, PCA bases from full 20 s clean segments were compared with bases from their last 10 s. Projector similarity, mean canonical correlation, and |PC1 dot| quantified similarity. Clean-vs-motion comparisons served as a discriminability check.

The primary endpoint was a paired absolute clinical-reference SV error. For each method comparison, complete-case paired windows were used. Reported values include medians, interquartile range (IQR) values, paired median deltas, percentage improved, and subject-level directional summaries. Because windows overlapped substantially due to the 5 s step, window-level p-values were treated as descriptive rather than confirmatory independent-sample inference. Subject-level analyses based on per-subject medians were used as conservative sensitivity checks but were power-limited by N = 6.

Baseline-error-dependent response was assessed by stratifying Cohort B into tertiles of WW-PCAICA SV error. Already-low-error maintenance was summarized by the proportion of windows with baseline SV error ≤10 mL that remained ≤10 mL after filtering. Large worsening was defined descriptively as CleanRef-PC1-10 SV error minus WW-PCAICA SV error greater than +5 mL or +10 mL.

References

1. Frerichs I, Amato MBP, van Kaam AH, Tingay DG, Zhao Z, Grychtol B, et al. Chest electrical impedance tomography examination, data analysis, terminology, clinical use and recommendations: consensus statement of the TRanslational EIT developmeNt stuDy group. Thorax. 2017;72:83-93.

2. Adler A, Boyle A. Electrical impedance tomography: tissue properties to image measures. IEEE Trans Biomed Eng. 2017;64:2494-2504.

3. Leonhardt S, Lachmann B. Electrical impedance tomography: the holy grail of ventilation and perfusion monitoring? Intensive Care Med. 2012;38:1917-1929.

4. Putensen C, Hentze B, Muenster S, Muders T. Electrical impedance tomography for cardio-pulmonary monitoring. J Clin Med. 2019;8:1176.

5. Yang L, Qu S, Zhang Y, Zhang G, Wang H, Yang B, Xu C, Dai M, Cao X. Removing clinical motion artifacts during ventilation monitoring with electrical impedance tomography: introduction of methodology and validation with simulation and patient data. Front Med. 2022;9:817590.

6. Jang GY, Jeong YJ, Zhang T, Oh TI, Ko RE, Chung CR, Suh GY, Woo EJ. Noninvasive, simultaneous, and continuous measurements of stroke volume and tidal volume using EIT: feasibility study of animal experiments. Sci Rep. 2020;10:11242.

7. Jang GY, Chung CR, Ko RE, Lee JY, Oh TI, Suh GY, Kim Y, Woo EJ. Real-time measurements of relative tidal volume and stroke volume using electrical impedance tomography with spatial filters: a feasibility study in a swine model under normal and reduced ventilation. Ann Biomed Eng. 2022;50:1141-1153.

8. Lee K, Jang GY, Kim Y, Woo EJ. Multi-channel trans-impedance leadforming for cardiopulmonary monitoring: algorithm development and feasibility assessment using in vivo animal data. IEEE Trans Biomed Eng. 2022;69:1964-1974.

9. Chung CR, Ko RE, Jang GY, Lee K, Suh GY, Kim Y, Woo EJ. Comparison of noninvasive cardiac output and stroke volume measurements using electrical impedance tomography with invasive methods in a swine model. Sci Rep. 2024;14:2962.

10. Dang TH, Jang GY, Lee K, Oh TI. Motion artifacts reduction for noninvasive hemodynamic monitoring of conscious patients using electrical impedance tomography: a preliminary study. Sensors. 2023;23:5308.

11. Chang CY, Hsu SH, Pion-Tonachini L, Jung TP. Evaluation of artifact subspace reconstruction for automatic artifact components removal in multi-channel EEG recordings. IEEE Trans Biomed Eng. 2020;67:1114-1121.

12. Behzadi Y, Restom K, Liau J, Liu TT. A component based noise correction method (CompCor) for BOLD and perfusion based fMRI. NeuroImage. 2007;37:90-101.

13. Senn A, Button D, Zollinger A, Hofer CK. Assessment of cardiac output changes using a modified FloTrac/Vigileo algorithm in cardiac surgery patients. Crit Care. 2009;13:R32.

14. Monnet X, Vaquer S, Anguel N, Jozwiak M, Cipriani F, Richard C, Teboul JL. Comparison of pulse contour analysis by Pulsioflex and Vigileo to measure and track changes of cardiac output in critically ill patients. Br J Anaesth. 2015;114:235-243.

15. Critchley LAH, Critchley JAJH. A meta-analysis of studies using bias and precision statistics to compare cardiac output measurement techniques. J Clin Monit Comput. 1999;15:85-91.

16. Bland JM, Altman DG. Statistical methods for assessing agreement between two methods of clinical measurement. Lancet. 1986;1:307-310.

17. Hyvärinen A. Fast and robust fixed-point algorithms for independent component analysis. IEEE Transactions on Neural Networks. 1999;10:626–634.

Funding

This research was supported by the National Program for Excellence in SW supervised by the IITP (Institute of Information & Communications Technology Planning & Evaluation) in 2026 (2023-0-00055) and also by the National Research Foundation of Korea(NRF) grant funded by the MSIT (Ministry of Science and ICT), Korea.

Authors Contributions

J.C. conceived the main research idea, designed and conducted the experiments, analyzed the data, and wrote the original draft. D.G. contributed to research discussions and helped refine the study idea. S.H. provided the dataset and data-analysis code, participated in idea discussions, and reviewed and edited the manuscript. M.A. supervised the study and provided overall research guidance. All authors reviewed and approved the final manuscript.

Data availability statement

The datasets generated and/or analyzed during the current available from the corresponding author on reasonable request.

Competing Interests

The authors declare that they have no competing interests.

Figure Legend

Figure 1. Clean-reference PCA pipeline for motion-contaminated cardiac EIT. Sliding windows were formed from multichannel EIT/contact-impedance data, artifact-positive targets were paired with preceding clean references, and clean-reference PCA projection was applied before ECG-guided cardiac extraction.

Figure 2. Baseline SV error versus SV-error change after filtering. Negative values indicate improved clinical-reference SV agreement after CleanRef-PC1-10, with the largest recovery concentrated in high-baseline-error windows.

Figure 3. Clean20 versus clean10 spatial-basis similarity. Clean10 retained the dominant clean-reference spatial structure relative to clean20, while clean-vs-motion comparisons showed larger basis differences.

Figure 4. Bland-Altman SV agreement for WW-PCAICA and clean-reference PCA. Clean-reference PCA narrowed descriptive limits-of-agreement width relative to WW-PCAICA, but remaining dispersion does not establish clinical interchangeability.

Table Legend

Table 1. Detector-level window composition by subject. Counts summarize target-only detector diagnostics before endpoint-specific complete-case filtering and are not the denominators for Tables 2–4.

Table 2. All-comers clinical-reference SV comparison using complete-case Cohort B observations.

Table 3. Baseline-error-stratified all-comers SV response to CleanRef-PC1-10 filtering.

Table 4. Direct paired clean10-vs-clean20 comparison on matched clean20-motion20 targets. N denotes window-level complete-case pairs for each metric. SV N differs from xcorr/NRMSE N because SV required finite clinical-reference matching and scaling, whereas morphology metrics did not.